[11] R. Wallace, "6 GHz Time domain measurement of fast transient events," in *Proc. IEEE Int. Symp. Electromagn. Compat.*, Anaheim, CA, Aug. 1992, pp. 460–463.

[12] K. Kawamata, S. Minegishi, A. Haga, and R. Sato, "Measurement of very-fast voltage rise curve due to gap discharge using coupled transmission lines in distributed constant system," *IEEE Trans. Instrum. Meas.*, vol. 46, pp. 918–921, Aug. 1997.

Experimental and FDTD-Computed Radiation Patterns of Cellular Telephones Held in Slanted Operational Conditions

Gianluca Lazzi, Shyam S. Pattnaik, and Om P. Gandhi

***Abstract*— The objective of this paper is to investigate, numerically and experimentally, the radiation patterns of various commercial cellular telephones held in a realistically slanted position relative to the head, to understand the performance of such devices for normal use conditions. The investigation has been performed with and without the human head model at an angle of 30° with respect to the vertical. To avoid the stair-step modeling of the cellular telephone for the finite-difference time-domain (FDTD) formulation, the head has instead been tilted forward by 30° and a transformation of coordinates in the FDTD calculation has been used to obtain the desired vertical and horizontal polarizations. We show that the FDTD method gives results that are in good agreement with measurements, both for shape and gain of the radiation patterns, for all of the considered mobile telephones that use several types of antennas. Generally, a decrease of the cellular telephone gain for the vertical component of the field has been observed as compared to the vertical configuration of the telephone and also a decrease in gain is obtained when the phone is held against the human head. Furthermore, it is shown that the FDTD method is capable of providing fairly accurate results even for radiation patterns at a slanted angle and modeling of realistic cellular telephones.**

***Index Terms*— Cellular telephones, dosimetry, FDTD, radiation patterns.**

I. Introduction

The wireless telephone market has grown rapidly in the last few years. The demands of highly efficient and compact devices that comply with the Federal Communication Commission (FCC) 1996 Safety Guidelines [1] is now more than ever a top issue. This rapid expansion has pushed the research toward the necessity of finding suitable methods capable of testing mobile devices for radiation pattern performance and safety concerns.

At this time, various research groups in the world seem to have focused on two methods: experimental measurements [2] and finite-difference time-domain (FDTD) [3], [4] computation [5]–[9]. While experimental measurements make use of the actual mobile telephone being tested, there is still a question on the appropriateness of representing the human head with simplified phantoms that for compliance testing include, at most, three to four tissue-type materials. The FDTD method, on the other side, has also been questioned on the relative lack of detailed representation of the actual wireless telephone though the human head can be modeled with an anatomically realistic heterogeneity. To remove this perceived deficiency, some recent work has successfully imported in the FDTD grid computer-aided design (CAD) telephone models [5] even though proof of accuracy of FDTD results for wireless telephone modeling has previously been presented for several configurations [6], [7].

In this paper, we focus our attention on the far-field radiation patterns of wireless telephones in presence and absence of the human head model. Some results on this issue have been presented in the past [8], [9]. In [10], we have considered experimental and numerical far-field patterns of telephones held vertically in presence and absence of the human head model. This configuration is not very realistic since telephones are often held slanted relative to the head. Both experimental and numerical methods now allow us to consider realistic positioning of the cellular telephone, thereby permitting the analysis of realistic cases of tilted positions of the telephone that may give results that differ considerably from those obtained with vertical cellular telephones. This is extremely important in the design process of a mobile telephone to test its performance for normal use conditions.

Numerical and experimental results show good agreement both for gain and shape of the radiation patterns. Some differences are ascribed to different head models used for the two methods that mainly create some differences in the depth of the nodes.

II. Numerical and Experimental Methods

The need to tilt the numerical head model instead of the telephone complicates the calculation of the radiation pattern slightly. The situation is depicted in Fig. 1. Fig. 1(a) shows the placement of the head and telephone models in the FDTD grid, while Fig. 1(b) shows the setup of the experimental conditions corresponding to the desired configuration.

The anatomically based model used for the computations has been described in our earlier publications (see e.g., [11]). This is a model with a resolution of $1.974 \times 1.974 \times 3$ mm derived from the magnetic resonance imaging (MRI) scans of a male volunteer. Fourteen tissue types have been identified in the model, including muscle, fat, skin, cartilage, nerve, blood, parotid gland, CSF, eye humour, sclera, lens, pineal gland, pituitary gland, and brain. The most recent properties available in the literature [13] have been assigned to each of the tissues. The head model has been tilted forward by 20°, 30°, and 45°, as needed [12], by using a "best fitting" technique. For the present calculations, we have chosen a 30°-tilt angle since this seems to correspond to a typical angle that people use to hold cellular telephones. The main reason we decided to tilt the head instead than the cellular telephone is that in this way, it is much easier to model the telephone accurately without resorting to staircasing. This is particularly important especially for the correct modeling of the antenna. Most of today's mobile telephone antennas involve components (such as helical antennas) that are very difficult to model with a tilted version of the handset.

An FDTD mesh of $153 \times 173 \times 140$ cells has been necessary for each simulation involving the human head model, while a mesh of $51 \times 68 \times 140$ has been adequate for the simulation of the handset in air needed for calculations of the radiation patterns in the absence of the head. The retarded time (RT) boundary conditions [14] have been used for all simulations.

In the experimental setup, the Utah heterogeneous model [15] has been used. The skull is simulated by 5–7-mm-thick KCl solution-laced epoxy composition, while the other tissues have been realized

Manuscript received June 15, 1998; revised February 5, 1999.

The authors are with the Department of Electrical Engineering, University of Utah, Salt Lake City, UT 84112 USA.

Publisher Item Identifier S 0018-9375(99)04091-0.

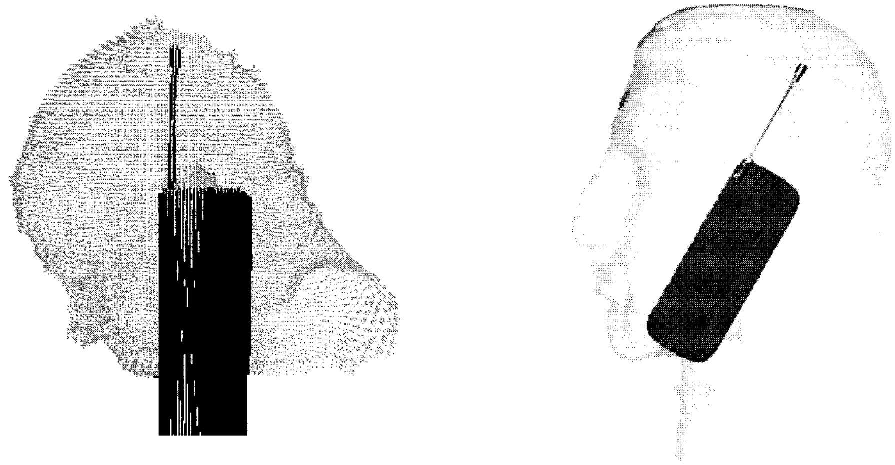

(a) (b)

Fig. 1. The setup used for the radiation pattern calculation. (a) Numerical. (b) Experimental.

by different compositions of water, salt, polyethylene powder, and the gelling agent TX 151.[1] The head is mounted on a turntable driven by a stepper motor as explained in [7]. The system is fully computer controlled and capable of displaying the measured radiation pattern in less than 8 min.

III. Results

For brevity, this section focuses on the results obtained for three representative telephones equipped with different antennas, even though results for several other telephones have also been obtained in our laboratory.

The first two telephones (referred to as device number 3) are equipped with monopole antennas of length 15 and 7.2 cm, respectively, while the third telephone (devices number 1) utilizes a whip antenna consisting of a helical part at its base and an upper monopole. The helical antenna has been modeled following the approach described in [10]. In this approach, the helix is replaced by a stack of equivalent electric and magnetic sources of appropriate relative weigths in order to reconstruct the near- and far-field generated by the helix. All the three telephones have the midband frequency of 835 MHz.

The telephones have been activated for the experimental measurements by using test mode. Therefore, no cables have been used to feed power in order to avoid any kind of interference or modification in their radiation patterns from normal use condition. The only problem of this approach is given by the fact that in some of the cases the actual radiated power from the cellular telephone is not known exactly. Moreover, often the radiated power of the actual telephones could be a function of the battery charge. The quantity that can be measured is the gain-power product (EIRP) and, therefore, the exact measure of the gain can be done only when the radiated power is known. Table I reports the EIRP and the gain of the vertical components of the telephones tilted at a 30° in air (in dBi) measured and FDTD-computed for an assumed radiated power of 600 mW for device numbers 1 and 3, and 380 mW for device number 2. For telephones numbers 1 and 3, 600 mW is the nominal radiated power given by the manufacturers, while for telephone number 2, the power quoted is the measured power delivered to the antenna as measured between forward and reflected power at the antenna terminals. Some of the difference in calculated and measured gain may therefore be due to the fact that the actually radiated power for experimental measurements is sligthly less than the assumed power.

[1] Available from Oil Center Research, P.O. Box 51871, La Fayette, LA.

TABLE I

Maximum Gain for the Three Considered Telephones in Air. The Handset is Positioned at a 30° Angle with Respect to the Vertical. Also Reported the Maximum Measured Gain-Power Product

Tel. No.	Measured or Assumed Power† (mW)	FDTD-Calculated Gain-Power Product (EIRP) (mW)	Measured Gain-Power Product (EIRP) (mW)	FDTD-Calc. Gain (dBi)	Measured Gain (dBi)
1	600	713.1	679.4	0.75	0.54
2	380	575.2	466.4	1.80	0.89
3	600	901.9	879.3	1.77	1.66

TABLE II

Maximum Gain for the Three Considered Telephones in the Presence of the Human Head. The Handset Is Positioned at a 30° Angle with Respect to the Vertical. Also Reported Is the Maximum Measured Gain-Power Product

Tel. No.	Measured or Assumed Power† (mW)	FDTD-Calculated Gain-Power Product (EIRP) (mW)	Measured Gain-Power Product (EIRP) (mW)	FDTD-Calc. Gain (dBi)	Measured Gain (dBi)
1	600	724.6	492.2	0.82	-0.86
2	380	377.4	350.6	-0.03	-0.35
3	600	635.5	520.2	0.25	-0.62

Table II gives the maximum vertical component effective isotropic radiated power (EIRP) and gain of the three telephones when they are held at an angle of 30° in presence of the human head. The aforementioned uncertainty in the actually radiated power is also valid in this case. Moreover, the shapes and compositions of the head models used for the measurements (homogeneously filled with tissue-simulant materials) and calculations (anatomically based with a 14-tissue composition) are different, which may partially explain the differences in maximum gain between measurements and computations. In addition, experimental gains could be lower since, in practice, the presence of the head affects the antenna matching, resulting in a lower actual power radiated from the telephone that

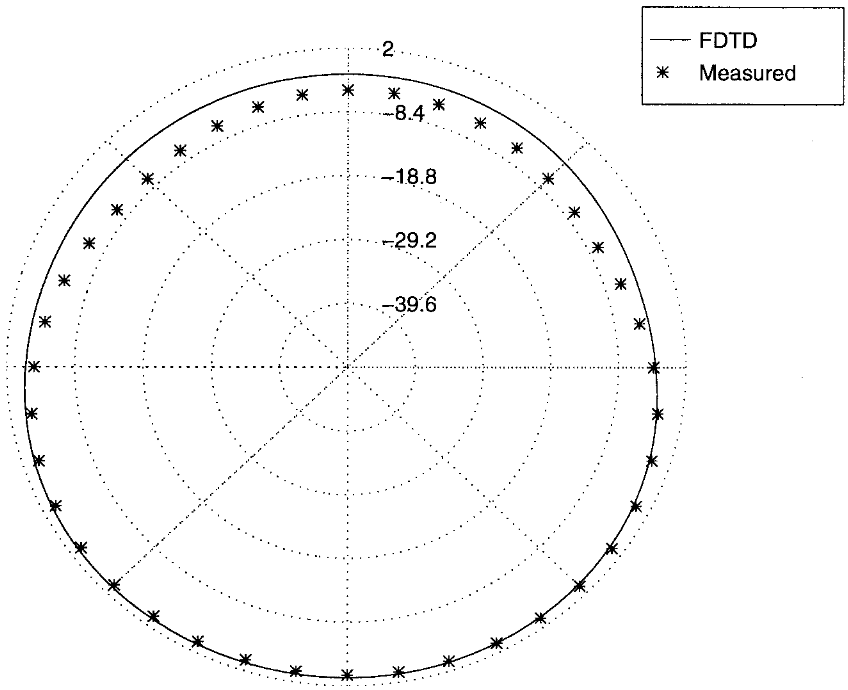

Fig. 2. FDTD computed and measured radiation pattern for telephone no. 1 in air. Tilt angle = $30°$.

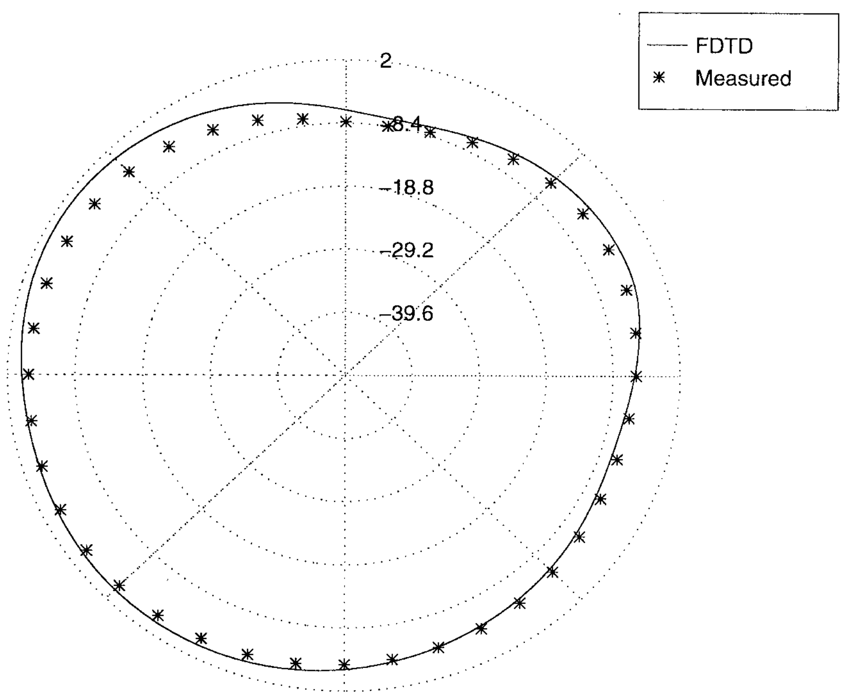

Fig. 3. FDTD computed and measured radiation pattern for telephone no. 1 in presence of the head model. Tilt angle = $30°$.

may contribute to increase the difference between experimental and FDTD computed results.

Fig. 2 shows the comparison between numerically computed and experimental vertical component of the radiation patterns for the telephone no. 1, in air. This radiation pattern is for the case of a 30° tilted handset. The two sets of data agree well both in gain and shape in all the directions. Compared to radiation pattern of the same telephone in air held in vertical position, we observed that tilting the phone caused a gain reduction in the first and second quadrants and a decrease in maximum gain of about 1 dBi.

The radiation pattern of this telephone is substantially affected in the presence of the human head model. Fig. 3 shows the comparison of the vertical component of the far field for telephone no. 1 held at a 30° angle against the vertically held human head model. The numerically calculated and measured radiation patterns agree extremely well. With respect to the case the of vertical held telephone and 30° tilted telephone, in the case of tilted handset we observed a lower gain for almost three quadrants.

IV. Conclusions

This paper investigates in detail the far field of actual cellular telephones held at a realistic position in proximity of the human head—numerically and experimentally. The telephones have been placed at a typical angle of 30° with respect to the vertical. The FDTD method and the measurement system provided results in good agreement, both in shape and gain of the radiation patterns, for all the considered mobile telephones equipped with various different antennas. We have observed a slight decrease of the cellular telephone performance with respect to the vertical position, while a sensible decrease in gain has been found when the phone is held against the human head. This investigation confirms that the FDTD method is a valuable technique to design cellular telephone antennas, being capable of providing accurate results even in challenging conditions involving radiation patterns at tilted angles and modeling of realistic cellular telephones. The technique could be extremely important in the design of mobile telephone since it allows to predict correctly the behavior of the telephone in normal use conditions.

References

[1] "Guidelines for evaluating the environmental effects of radiofrequency radiation," FCC 96-326, Aug. 1, 1996.

[2] Q. Balzano, O. Garay, and T. J. Manning, Jr., "Electromagnetic energy exposure of simulated users of portable cellular telephones," *IEEE Trans. Veh. Technol.*, vol. 44, pp. 390–403, 1995.

[3] K. S. Kunz and R. J. Luebbers, *The Finite-Difference Time-Domain in Electromagnetics.* Boca Raton, FL: CRC, 1993.

[4] A. Taflove, *Computational Electrodynamics: The Finite-Difference Time-Domain Method.* Dedham, MA: Artech House, 1995.

[5] A. D. Tinniswood, C. M. Furse, and O. P. Gandhi, "Computations of SAR distributions for two anatomically-based models of the human head using CAD files of commerical telephones and the parallelized FDTD code," *IEEE Trans. Antennas Propagat.*, vol. 46, pp. 829–833, June 1998.

[6] P. Bernardi, M. Cavagnaro, and S. Pisa, "Evaluation of the SAR distribution in the human head for cellular phones used in a partially closed environment," *IEEE Trans. Electromagn. Compat.*, vol. 38, pp. 357–366, 1996.

[7] G. Lazzi and O. P. Gandhi, "On modeling and personal dosimetry of cellular telephone helical antennas with the FDTD code," *IEEE Trans. Antennas Propagat.*, vol. 45, pp. 525–530, Apr. 1997.

[8] M. A. Jensen and Y. Rahmat-Samii, "EM interaction of handset antennas and a human in personal communication," *Proc. IEEE*, vol. 83, pp. 7–17, 1995.

[9] M. Okoniewski and M. A. Stuchly, "A study of the handset antenna and human body interaction," *IEEE Trans. Microwave Theory Tech.*, vol. 44, pp. 1855–1864, Oct. 1996.

[10] G. Lazzi, S. S. Pattnaik, C. M. Furse, and O. P. Gandhi, "Comparison of FDTD-computed and measured radiation patterns of commercial mobile telephones in presence of the human head," *IEEE Trans. Antennas Propagat.*, vol. 46, pp. 943–944, June 1998.

[11] O. P. Gandhi, G. Lazzi, and C. M. Furse, "Electromagnetic absorption in the human head and neck at 835 and 1900 MHz," *IEEE Trans. Microwave Theory Tech.*, vol. 44, pp. 1884–1897, Oct. 1996.

[12] G. Lazzi and O. P. Gandhi, "Realistically tilted and truncated anatomically based models of the human head for dosimetry of mobile telephones," *IEEE Trans. Electromagn. Compat.*, vol. 39, pp. 55–61, Feb. 1997.

[13] C. Gabriel, "Compilation of the dielectric properties of body tissues at RF and microwave frequencies," Armstrong Lab. Tech. Rep. AL/OE-TR-1996-0037, Occupat. Environmental Health Directorate, RFR Div., Brooks AFB, TX, June 1996.

[14] S. Berntsen and S.N. Hornsleth, "Retarded time absorbing boundary conditions," *IEEE Trans. Antennas Propagat.*, vol. 42, pp. 1059–1064, Aug. 1994.

[15] O. P. Gandhi, J. Y. Chen, and D. Wu, "'Electromagnetic absorption in the human head at 835 and 1900 MHz," in *Proc. Int. Symp. Electromagn. Compat.*, Rome, Italy, Nov. 1994, pp. 1–5.

Loop-Shield-Loop Shielding Effectiveness

R. C. Hansen and J. Ronald Moser

***Abstract*—The 1967 formulation by Moser of the shielding effectiveness of a metal sheet on a small loop is extended to loop-to-loop coupling. The integration of flux through the receiving loop simply adds another $J_0(ka)$ Bessel function to the Moser integrands; the result is a monotonic variation of coupling with loop spacing, unlike the original results.**

***Index Terms*—Antennas, electromagnetic coupling, loops, near fields, shielding effectiveness.**

I. Introduction

Electromagnetic shielding of rooms or equipment through use of metal walls or sheets has been important for many decades and is now even more necessary with the burgeoning number of RF transmitters of all types. For plane wave sources, there are well-known simple formulas for transmission through a metal sheet or through a multiple layer wall, using A-B-C-D or equivalent chain matrices. Often, the frequencies of interest are sufficiently low that the metal wall is in the near field of a source or a test antenna. For these cases, the shielding effectiveness (SE) may be significantly different than for the plane wave case.

Moser [1], in a classic paper obtained the SE of a metal wall when the source antenna is an electrically small loop and when the wall is in its near field. The loop magnetic field was expanded into an integral of plane waves; each plane wave component could then be propagated through the wall. The result is a quotient of two integrals involving the J_1 Bessel function. Computations were performed by Ryan [2] for two thicknesses of copper, aliminum, and steel walls. Suffice it to say here that excellent agreement existed with measurements; these will be discussed later. Approximate formulas for thin and for thick walls (in skin depths) were given by Bannister [3], [4].

Although Moser formulated the exact near-field produced by the loop and shielding metal wall, the shielding effectiveness formula gave field on the transmitting loop axis. When calculations (described later) are made versus loop-observation point spacing, the shielding shows a "bathtub" shape, that is a minimum shielding occurs for spacing comparable to loop radius. Of most practical interest, however, is coupling between two identical loops; this requires an integration of flux through the receiving loop. In this paper, the modified Moser shielding effectiveness formula is given and results are compared with those from the earlier formula.

Manuscript received June 11, 1996; revised February 9, 1999.

R. C. Hansen is with R. C. Hansen, Inc., Consulting Engineer, Tarzana, CA 91357 USA.

J. R. Moser is at Garland, TX 75041 USA.

Publisher Item Identifier S 0018-9375(99)04089-2.